Pore-scale comparisons of primary drainage techniques on non-water-wet reservoir rocks

Franck Nono[1,*], *Fabrice* Pairoys[2], *Victor* Fernandes[2], *Cyril* Caubit[2]

[1]Akkodis, 64000 Pau, France
[2]TotalEnergies, 64000 Pau, France

Abstract. Initial water saturation (S_{wi}) is a critical parameter that significantly influences multiphase flow properties, wettability, and the prediction of reservoir dynamics during fossil fuel energy recovery, Non aqueous phase liquid (NAPL) depollution or CO_2 storage campaigns. In a recent study [1], we investigated the differences between the commonly used initialization methods and the impact of various laboratory protocols on achieving S_{wi}, at the pore scale. The study primarily focused on the primary drainage of water-wet Bentheimer sandstones with some preliminary observations made on initial non-water-wet Bentheimer samples. The study revealed several unexpected artifacts.

Building upon the previous work, the present study employs 3D X-ray microtomography to extend the investigations to reservoirs rocks that are not water-wet at the beginning of primary drainage. Specifically, the porous plate (PP) and oil flooding (OF) techniques are the focus. The study examines S_{wi} average values and profiles, pore occupancies and effective permeabilities. Several key observations are made: (i) The porous plate always leads to lower S_{wi} values than the oil flooding technique even when both techniques are performed with the same inlet pressures. It is argued that these differences may depend on both the pressure build-up till the saturation front which is higher for the porous plate technique compared to the oil flooding technique, or the reversal flow which may re-inject trapped fluids from the diffusers' dead volumes into the sample. The latter is mainly function of the rock's wettability regarding the invading fluid [2], (ii) the study highlights the differences in pore occupancies when comparing different initiation methods on oil-wet reservoir rocks. Important parameters to consider here are how wettability is initially distributed in the sample and the connectivity of the macropores.

The findings highlight the not so well expected complexities associated with S_{wi} initialization, pore occupancies, and flow behaviour. Understanding these aspects is crucial for accurate reservoir characterization and improved decision-making in oil and gas exploration and other related applications and the DRP tool can provide insights to predict these behaviours.

1 Introduction

The forecast of the flow behaviour in underground reservoirs requires the knowledge of important properties such as relative permeability and capillary pressure, which are relevant to the recovery processes that will be implemented whatever the purpose (e.g., CO2/H2 storage, fossil fuel recovery, soil remediation, etc.). These properties are obtained through core-scale laboratory experiments using techniques and protocols that closely mimic the flow processes in reservoirs.

One key step common to these experiments is the establishment of initial water saturation, referred to as S_{wi} ("i" for initial) or S_{wirr} ("irr" for irreducible), depending on the presence of mobile water saturation. There are various laboratory techniques available to initialize reservoir cores at a targeted S_{wi}, and as documented in [1], they exhibit significant discrepancies. The major concerns in this area arise from 3 main aspects.

The first point of divergence arises from whether to use native state or restored state samples in laboratories for core flooding experiments. It is well acknowledged that all reservoir rocks were initially water wet, and the wettability is altered afterwards during oil migration in oil & gas reservoirs. This alteration occurs over millions of years due to the interaction between crude oil, formation brine and reservoir rock under high pressure and temperature conditions. Therefore, it could be argued that working with native state cores helps maintain the exact reservoir wettability. However, this approach is known to be challenging and presents potential drawbacks such as the impact of mud invasions [3, 4], or changes in fluids distribution during coring due to pressure-temperature variations. The restored state method is generally the preferred approach [4]. In this method, samples undergo solvent cleaning to remove fluids and restore the cores to a water wet state, similar to the reservoir before oil migration. This is followed by primary drainage and aging steps to restore the final reservoir wettability and the initial fluids saturation. Although there is more control over the different states of the cores during these steps, issues related to the inefficiency of the cleaning process are often encountered [4, 5], especially for rocks containing organic matter such as pyrobitumen and coal, or rocks that have been

* Corresponding author: franck.nono-nguendjio@akkodis.com

contaminated with drilling muds [4]. In such cases, wettability may affect the distribution of primary drainage S_{wi} [1, 6]. A premise of demonstration has been achieved by [1] on a well-known water-wet outcrop, where the initial wettability was artificially altered to oil wetness using a silane treatment. The authors observed, through 3D X-ray microtomography, large blobs of brine trapped in big pores after primary drainage. This observation is inconsistent with water-wet primary drainage. However, the question arises whether this phenomenon occurs in real reservoir rocks, considering that the silane treatment creates an artificial and uniform wettability distribution, which is not the case in reservoir rocks [7, 8].

The second point of divergence comes from the different primary drainage methods themselves. Various initialization methods exist, including centrifugation, porous plate, and the oil flooding methods which are the most used. A review of the literature reveals significant discrepancies between these methods [1, 9], with one of the main artifacts being the presence of capillary end-effects during oil flooding or centrifugation on water-wet samples. The porous plate is considered the most robust method but is time-consuming and expensive. A recent technique was developed [10] that addresses the weaknesses of the traditional methods for water-wet plugs. It combines the speed of the oil flooding and the robustness of the porous plate in an overall workflow. However, regarding primary drainage on oil-wet samples, which is often observed, there is no clear indication in the literature. Nono *et al.* [1] recently observed different patterns when achieving primary drainage through oil flooding or using a porous plate on artificial oil wet Bentheimer sandstone. The porous plate method appeared to decrease the S_{wi} much easier compared to the oil flooding, yet with a higher value than that of water wet samples, but surprisingly closer pore occupancy to a water-wet case. In contrast, oil flooding exhibited the expected trapping of large blobs of brine in big pores.

The third point of divergence is related to the core flooding protocols within different laboratories. Even when using the same primary drainage method, the implemented protocols can yield vastly different results. For example, Nono *et al.* [1] demonstrated that reversing the flow in centrifuge and oil flooding experiments to flatten the saturation profile during primary drainage leads to the disconnection of non-wetting phase clusters, thereby impacting wettability alteration and homogeneity.

Many of these issues are now well documented in the literature [1, 2, 11, 12] and attempts to resolve them have led to optimized apparatuses [10, 13]. However, most investigations have been conducted on water-wet rocks, and only a few studies have explored rocks with altered wettability, which represents a significant aspect of the real situation in laboratories.

In this study, we extend our previous investigations [1] to include reservoir rocks known to exhibit non- water-wet characteristics after a conventional cleaning, either due to pyrobitumen coating or the presence of organic matter. It should be noted that the observations presented in this paper can be extrapolate to rocks that are not well cleaned or rocks that are contaminated with drilling muds. To achieve the objectives of this study, we employed 3D X-ray microtomography to directly observe the fluids within the pore network.

2. Materials and methods

2.1. Porous media

Two reservoir rocks, designated as rock A and rock B, were selected for this investigation. The selection of these reservoir rocks was based on their SEM analysis, which revealed the presence of significant amounts of heavy oil fractions remaining in the pore network even after undergoing conventional cleaning procedures. The mineralogy and pore-throat size distributions of these rocks are provided in Table 1 and depicted in figure 1, respectively.

Table 1. Mineralogy of the rock types used in this study

Rock A	**85% Quartz** – **6% Calcite** – 6% Micas – 1% Kaolinite
Rock B	**3 % Quartz** – 0.5% K Feldspar – **8.8% Calcite** – **86% Dolomite** – 0.2% Pyrite – **1.5% Total Clay** – 1% Mica – 0.5% Smectite

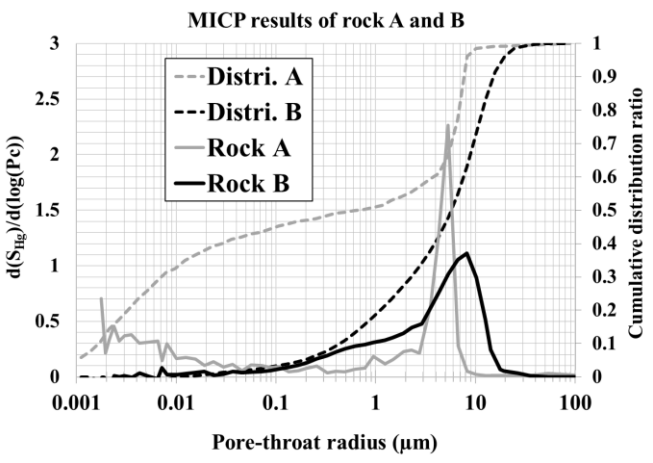

Fig. 1. Pore-throat size distributions and cumulative frequencies of rock A and B determined through MICP experiments.

In this study, primary drainage experiments were conducted on a total of 4 samples: three mini-plugs from rock A and one mini-plug from rock B. For rock A, the methodology followed was the same as in [1], with the aim of targeting low and high S_{wi} using porous-plate (PP) and the oil flooding (OF) methods. The flooding methodology mainly consisted in: (i) increasing gradually capillary pressure till the desired initial water saturation for the PP technique, (ii) increasing gradually the capillary number (drainage flowrate) till the desired S_{wi}. At the end of this process, we reverse the flow using only the highest flowrate achieved in the previous direction. First trials achieved on twin mini-plugs and the SCAL laboratory drainage capillary pressure results helped us to narrow our capillary number and capillary pressure ranges to obtain our S_{wi} targets.

For rock B, only one sample was used as it was not possible to target very low S_{wi}. On this sample, both oil flooding and

porous plate methods were performed. All the plugs were trimmed to a length of 2 cm.
For the sake of clarity when talking about porosity, we refer to "sub-porosity" as the porosity that is below the spatial resolution of our microtomography (unresolved porosity). The part of the porosity that we clearly see (resolved) will be called the "Macro-porosity". The total porosity will directly be the sum of the Macro-porosity and the Sub-porosity.
In the same way, total S_{wi} will be the sum between S_{wi} in Sub-pores and S_{wi} in Macro-pores. The characteristics of the samples used in this study are provided in table 2.

Table 2. Samples characteristics

Sample	D mm	K_w mD	Total porosity %	S_{wi} %	S_{wi} in Sub-pores %
A-OF1	3.96	54.1	21.4	4	4
A-OF2	3.94	40.5	22	50	39.6
A-PP	9.9	70.1	19	46 and 7	43 and 7
B-PP & B-OF (same plug)	3.96	11.8	11.6	**29.6** & 39.3	**25.9** & 23

2.1.1 Reservoir rock A

Reservoir rock A is primarily composed of Quartz (85%), with a small proportion of Calcite.
It displays a unimodal pore-throat size distribution, with the peak value around 5.3 µm. 3D images acquired on our Zeiss Versa 520 microtomography device were 2µm to 5µm of voxel size resolution meaning that a part of our porosity will be unresolved.
Figure 2 illustrates the spatial distribution of macropores and unresolved pores on a 2D cross section of a mini plug A. The investigated permeabilities range from 40mD to 70mD and porosities vary between 19.0% and 21.4%.
It should be noted that a significant amount of the porosity falls below the resolution of the images, referred as sub-porosity.

resolved porosity, generally exhibit homogeneity (examples shown in figure.3). We performed a cluster analysis on the visible porosity of mini plugs from rock A. With our image processing tool, we can count the number of disconnected clusters, determine their volumes, areas and also evaluate their morphology. We should note that these values are directly impacted by the image resolution. Higher is the resolution, more we capture thinner features and connections.

We evaluated the connectivity of the resolved porosity (macroporosity). By connectivity, we mean what is the fraction of the largest cluster of the macroporosity on the overall macroporosity in terms of volume. We found that at 2µm image resolution, the resolved largest cluster represented 70% of the overall macroporosity whereas at it represented only 30% of the overall macroporosity at 5µm image resolution. This means that our macroporosity is quite well defined and connected at 2µm voxel resolution whereas we lose a lot of connections when going down to 5µm of voxel resolution.

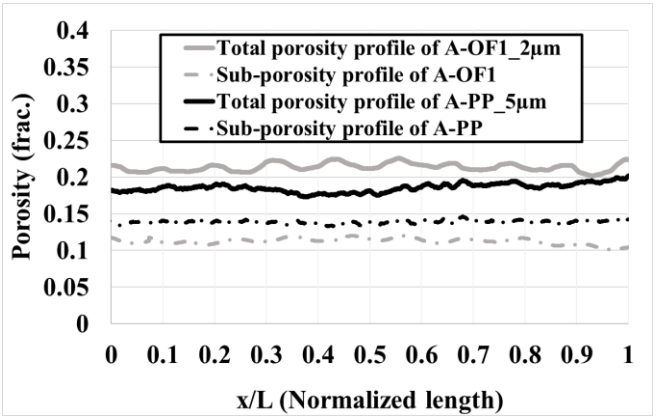

Fig. 3. Examples of porosity profiles of rock A plugs. Dashed lines represent sub-porosity profiles and solid lines represent the total porosity profiles. The 2 samples were acquired at different image resolutions: 2 and 5 µm, thus different amount of sub-resolved porosity.

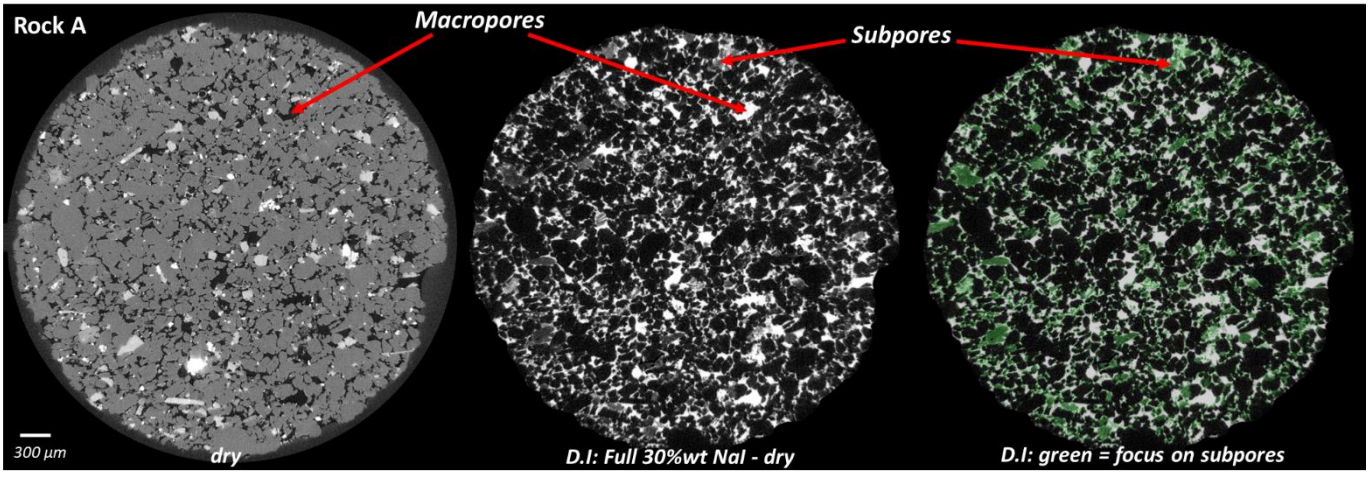

Fig. 2. Illustration of the spatial distribution of macropores and sub-pores using Differential Imaging (D.I) methodology [14] on a mini plug from rock A.

Through 3D image processing, it was determined that the porosity profiles, both in the visible-porosity and the sub-

SEM images (shown in figure.4) conducted on a cleaned sample revealed the presence of patchy coatings of organic

components scattered throughout the surface of clean cements (Quartz and calcite) in the macropores. These coatings consist of sedimentary organic fragments and amorphous deposits that remain in the pore network even after undergoing conventional cleaning procedures.

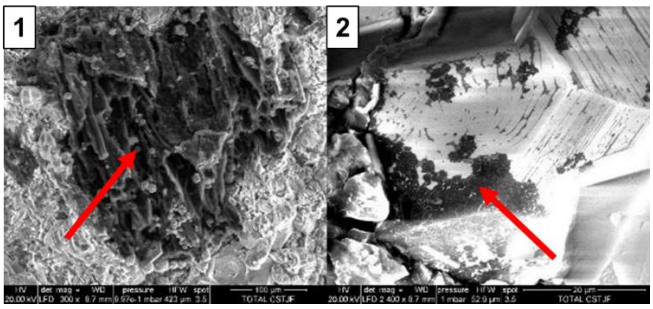

Fig. 4. SEM images of rock A acquired within TotalEnergies' SEM-FEG Quanta 650. (1) shows the fibrous organic matter relative to the sedimentary fragment and (2) shows the amorphous deposits on a Quartz grain.

These observations confirm that the sample is not water-wet prior to primary drainage.

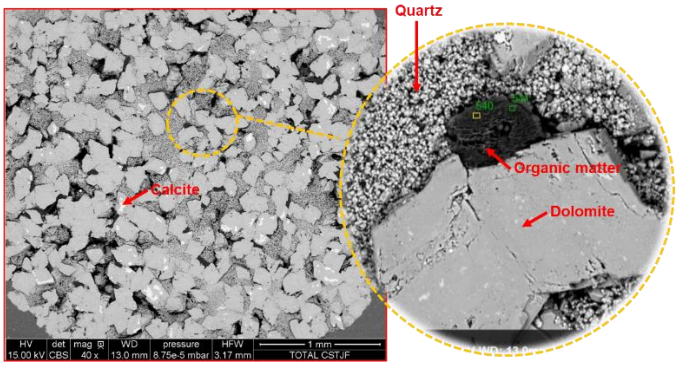

Fig. 6. SEM images of rock B acquired with SEM-FEG Quanta 650. Organic matter representing sedimentary fragments are also observed in this sample.

The quartz zones in this sample are clearly micropores locations. The total porosity and sub-porosity profiles (figure .7.) have some variations within 5% amplitude. The sample exhibits a macro-porosity at 2µm which has a connectivity of 66%. This connectivity at 2µm resolution is closer to rock A connectivity at the same pixel size.

2.1.2 Reservoir rock B

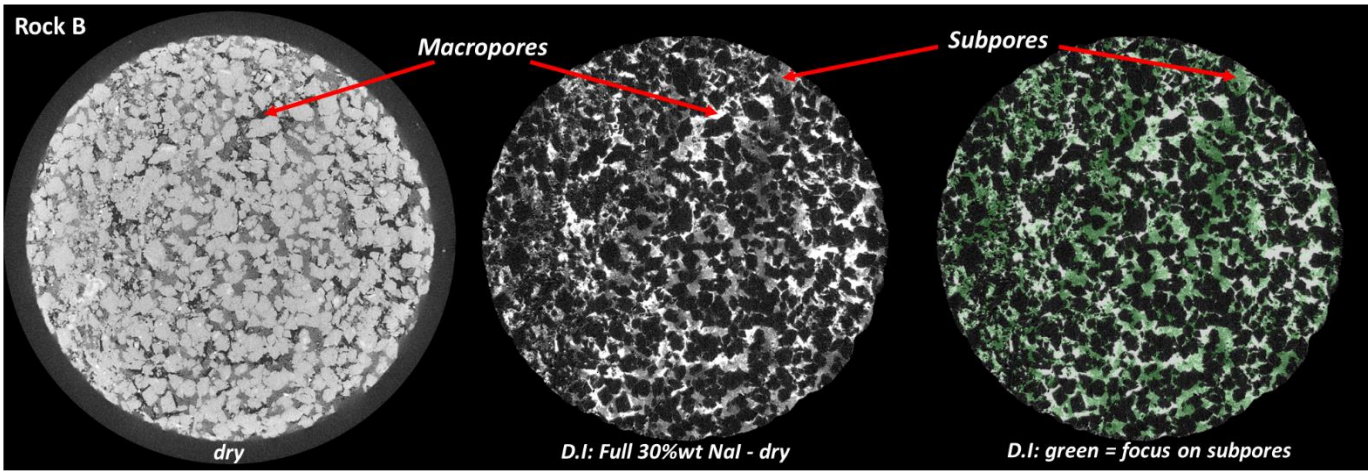

Fig. 5. Illustration of the spatial distribution of macropores and sub-pores using Differential Imaging (D.I) methodology [14] on a mini plug from rock B.

Reservoir rock B is predominantly composed of Dolomite + Calcite, accounting for 95% of the composition, with a small proportion of Quartz (3%).

Figure 5 illustrates the spatial distribution of macropores and unresolved pores on a 2D cross section of mini plug B.

The peak pore-throat radius in rock B is approximately 8µm (as seen in figure.1.) with absolute permeabilities averaging tens of millidarcies range, and porosities averaging around 10%.

As depicted in figure 6, there is also a presence of organic matter dispersed throughout the pore space. SEM images revealed similar findings to those observed in rock A; with sedimentary fragments remaining after the conventional cleaning. Additionally, a small portion of pyrobitumen material was detected, coating certain areas of the pore surface.

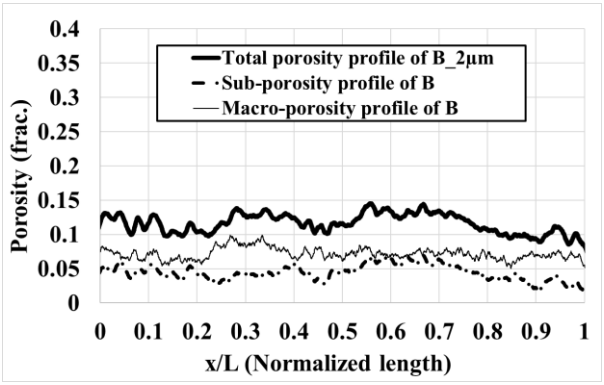

Fig. 7. Porosity profile of a rock B determined through 3D image processing. 3D images are acquired at 2 µm of resolution.

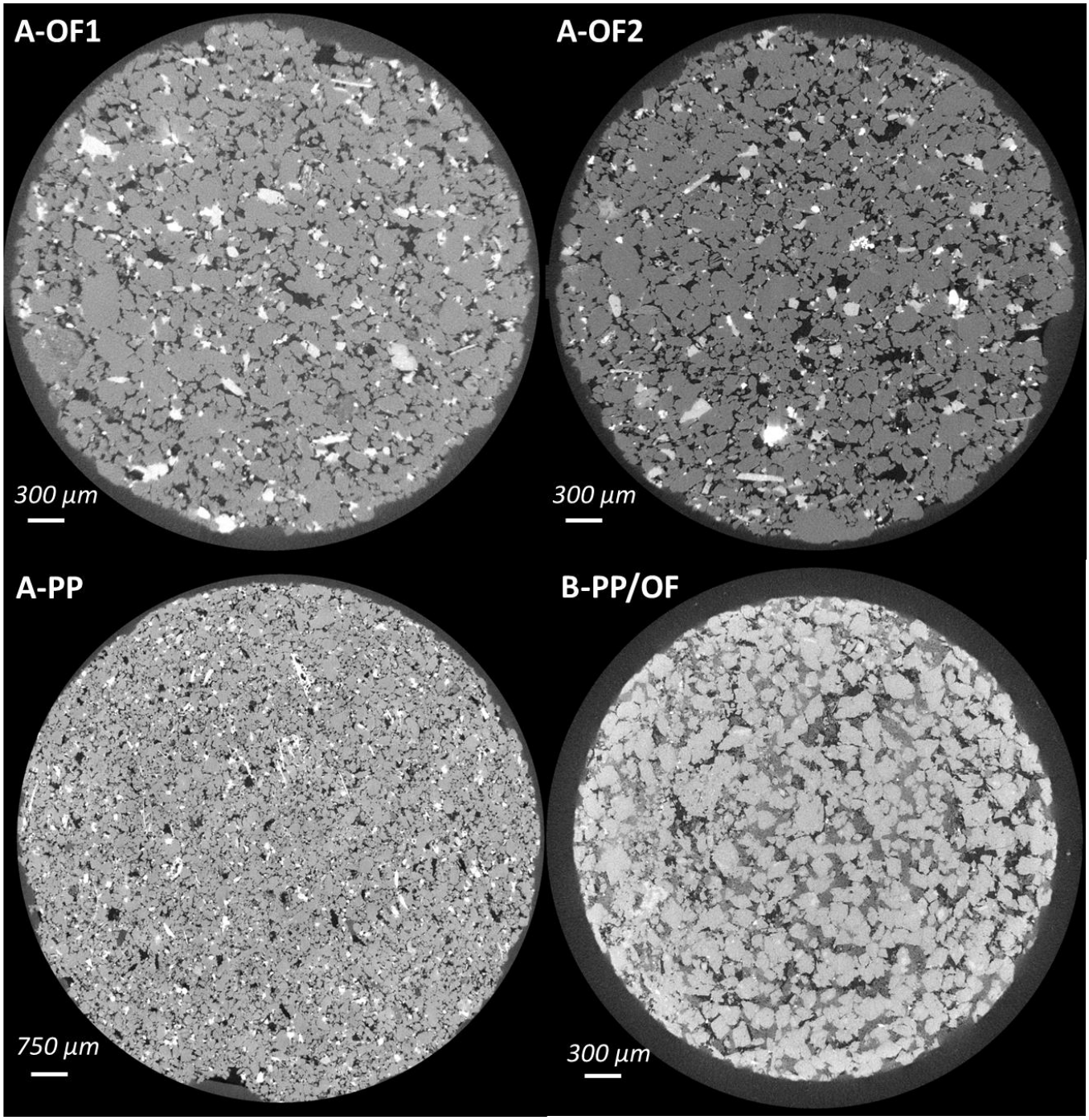

Fig. 8. 2D cross sections of mini plugs from rock A and the mini plug from rock B, used in this study

In figure 8 are depicted cross sections of all the plugs used in this study. A-OF's and B-OF plugs are acquired at 2µm resolution (4mm diameter plugs) where as A-PP is acquired at 5 µm resolution (1cm diameter plug).

2.2 Fluids

In this study, we specifically focused on primary drainage without any wettability alteration. We used a mineral oil: Marcol52 (μ_{M52} = 10 cP, and ρ_{M52}=0.83g.cc^{-1} at 25°C). For the brine phase, we used distilled water that was doped with 30%wt of Sodium Iodide. This doping increases the contrast between oil and brine for a better accuracy in image segmentation. It also allows quantifying the porosity on unresolved pixels of the images [14] and track brine saturation in the unresolved porosity using the differential imaging technique [15]. The IFT between both fluids is 42 mN.m^{-1}.

2.3 Image acquisition and processing

We utilized a Zeiss Xradia Versa 520 microtomograph to acquire the 3D X-ray images. Energy and power settings were respectively 90kV and 8W. For rock A, the voxel size varied between 2 µm and 5 µm. This variation is related to the diameter of the sample used: 4mm diameter for 2µm

resolution and 1cm diameter for the 5µm resolution. For rock B, the voxel size was 2 µm.
For 2µm resolution images, the field of view (FOV) was about 4 to 4.5 mm size. It means we could not acquire the entire length of the sample in one acquisition. We could just acquire a 4 to 4.5mm segment of the plug. To have the entire length, we needed a total of 6 segments (6 acquisitions) with an overlap between the segments. These segments are then stitched in an internal 3D reconstruction software and the outcome from this stitching is one global 3D volume of the 2cm length plug.
In terms of acquisition time, the total acquisition time for all the 6 segments would take approximately 24h, with an average of around 4 hours per segment.
The image processing was performed using both Avizo 2020.3® and ImageJ software.

2.4 Experimental set-ups

We used similar set-ups to those described in [1]. The flow experiments were conducted vertically, following the direction of gravity. For the 4 mm diameter plugs, flow properties could be measured during oil flooding experiments but not during porous plate experiments.
For the 1 cm diameter plugs cell, we were able to measure flow properties in both oil flooding and porous plate experiments, thanks to an optimized cell design as outlined in [1]. In all experiments, the confining pressure was set to 30 bars, and the pore pressure was maintained at 10 bars.

2.5 Experimental procedures

The experimental procedure is focused solely on primary drainage since crude oil was not used. The step-by-step protocol followed is as follows:

(i) Conventional cleaning of the mini plug at reservoir temperature following the cleaning procedure described in [1]
(ii) Dry 3D scanning of the sample along its entire length
(iii) Vacuum saturation of the sample with highly doped brine, followed by flushing at a low rate with 40 pore volumes (PVs). If possible, measurement of the absolute permeability is conducted during this step.
(iv) 3D scanning of the fully saturated sample with the doped brine.
(v) Primary drainage with Marcol52 using either the oil flooding technique (OF) or the porous plate (PP) till the target S_{wi}. In this study, we have chosen to follow a common laboratory approach which is to use a gradual increase of capillary numbers (for OF) or capillary pressure values (for PP) till S_{wi}. For the oil flooding method, at the end of the maximum capillary number, the flow is reversed to flatten the saturation profile. If possible, the effective oil permeability at S_{wi} ($K_o(S_{wi})$) is measured.
(vi) 3D scan of the entire sample saturated at S_{wi}.

Flowrates in this study are reported in terms of capillary number (Ca) which is calculated using equation 1:

$$C_a = v.\mu/\gamma \quad (1)$$

Where v represents the superficial fluid velocity ($m.s^{-1}$), γ the interfacial tension ($N.m^{-1}$) and μ the displacing phase viscosity (Pa.s).
4 samples are analyzed in this paper (see Table 2):

A-OF1: rock A sample targeting a low S_{wi} using oil flooding

A-OF2: rock A sample targeting a high S_{wi} using oil flooding

A-PP: rock A sample on which primary drainage is performed using the porous plate method at 2 capillary pressure values: low and high P_c (respectively for high and low S_{wi})

B-OF / **B-PP**: rock B sample undergoing primary drainage using the oil flooding technique first (B-OF). After a fast ambient cleaning to remove the fluids, the same sample is re-used for primary drainage using the porous-plate technique (B-PP). The main purpose here is to compare both techniques on the same sample since targeting low values of S_{wi} was not possible with the oil flooding method.

3 Results and discussions

In the analysis of the results, a separate investigation is conducted for each sample. For rock A, we will separate the comparisons on low and high S_{wi} targets. For rock B, as we were not able to reach low S_{wi} targets, the comparisons will be focused on the high targets obtained.

3.1 Results on rock A

3.1.1 Low targets of S_{wi} (A-OF1 and A-PP)

S_{wi} obtained in both experiments are very low (see Table 2). The porous plate experiment demonstrated a uniform saturation profile (figure 9). Oil flooding result exhibits some little heterogeneities on saturation profiles but remains very low without any noticeable capillary end-effect. Notably, the macro-porosity did not contain any brine, with the remaining brine being confined to the sub-porosity in both samples (Table 2).
These low S_{wi} values were achieved using a maximum capillary number close to 10^{-5} and a maximum capillary pressure of 6 bars.

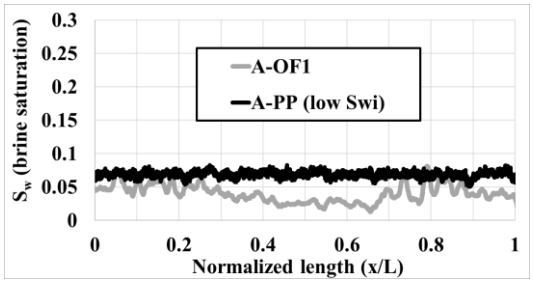

Fig. 9. Saturation profiles after primary drainage targeting low S_{wi} on rock A samples, using Oil flooding (OF) and Porous-plate (PP) techniques.

To further confirm the non-water-wet initial wettability of rock A, a waterflooding experiment was conducted on sample A-OF1 immediately after primary drainage at a capillary

number of Ca = $1.4.10^{-7}$. The images of the macro-pores (figure 10a) show oil (depicted as black) in small pores and corners while brine (light grey) occupies larger pores. The global saturation profile (figure 10b) and the macropores occupancies (figure 10c) were investigated. To extract the macropores network characteristics, we used the GNExtract algorithm developed with Imperial college of London [16].

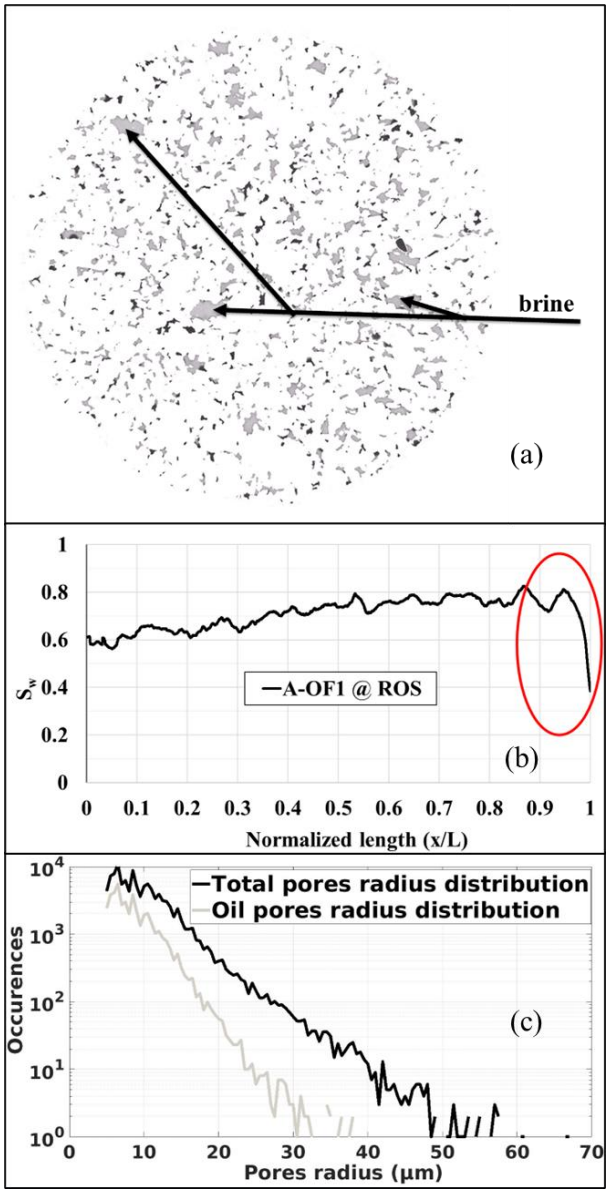

Fig. 10. Sample A-OF1 after waterflooding: (a) Macro-porosity image - Grains and Sub-porosity have been masked (white). The rest (black = oil and grey = water) represents the fluids in macropores, (b) Waterflooding saturation profile with the capillary end effect to oil at the outlet, (c) pore occupancies after waterflood of rock A, at ROS (remaining oil saturation)

The waterflooding saturation profile (figure 10b) clearly exhibits an end-effect to oil near the outlet face of **A-OF1** providing further evidence of the non-water-wet nature of rock A's macro-porosity. The results from pore occupancy analysis (figure 10c) align with this observation, showing that oil tends to occupy smaller pores while brine is present in larger pores. This contradicts the behavior expected in a water-wet system.

It is noteworthy that the observation during primary drainage in this study differ from those reported by [1] on artificially oil wet modified Bentheimer sandstone using a silane treatment. In this study, it was relatively easy to achieve very low S_{wi} values on rock A using the oil flooding technique without observing brine trapping in large pores, which contrasts with the modified Bentheimer case. It should be mentioned that the primary drainage protocols employed in this study were the same as those used in [1].

The saturation profile obtained through the porous plate technique shows a flat distribution compared to the oil flooding saturation profile. It is important to note that the sample used for the porous plate experiments had a larger diameter (1cm) compared to the oil flooding experiments (4mm). Therefore, local heterogeneities may have a greater influence on the smaller sample. However, these minor differences do not diminish the fact that both the oil flooding and porous plate techniques were able to achieve very low S_{wi} values on an initially non-water-wet rock, with brine present in the sub-resolved porosity (small pores) resembling a water-wet behaviour. This suggests that the sub-resolved porosity may exhibit a different wettability compared to the macro-porosity, at least in terms of being less oil wet. Further insights will be gained in subsequent sections when targeting higher S_{wi} values.

3.1.2 High targets of S_{wi} (A-OF2 and A-PP)

Water saturation profiles for both the macro-porosity and the total porosity for the two samples are depicted in figure 11.

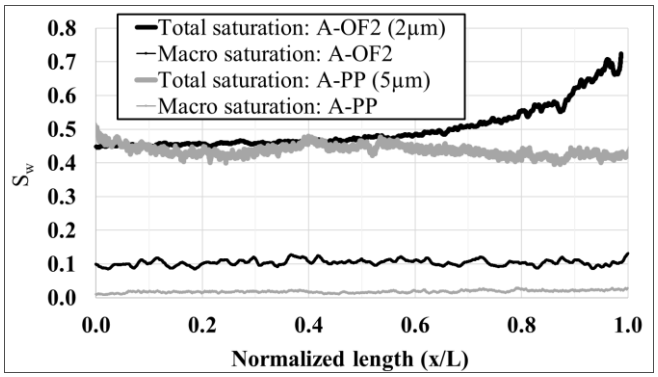

Fig. 11. Primary drainage saturation profiles of rock A targeting high S_{wi} values using OF and PP techniques

The discrepancy in S_{wi} values in macropores between OF and PP is mainly attributed to the voxel size of each experiment. The PP technique, conducted on a 1cm diameter plug, necessitates a voxel size of 5µm, while the OF technique, performed on a 4mm diameter sample, utilizes a voxel size of 2µm. As a result, some macropores that are visible at 2µm resolution may remain unresolved at 5µm resolution, leading to a decrease in macropore S_w for the 5µm voxel size images. Furthermore, a water-wet capillary end-effect is observed in the overall saturation profile of A-OF2. However, the saturation profile of the macropores remains constant (figure 11), indicating that this capillary end-effect originates from

the sub-resolved porosity. This finding confirms that the sub-porosity of rock A exhibits water-wet characteristics. Regarding the impact of flow reversal, it is difficult to draw conclusions about the disconnection of oil clusters in the macropores for the OF technique, as the brine in macropores could still be connected to the brine in the sub-pores. However, as observed, capillary end-effects persist and influence the saturation profile even after the flow reversal.
In contrast, the saturation profile obtained from the porous plate experiment (A-PP) remains flat in both the macro-pores and the sub-pores.
In summary, the main observations in this section are as follows: (i) most of the brine in the sample is retained in the sub-porosity, (ii) capillary end effects are observed in the sub-pores and impact the overall saturation profile even after the reversals in the OF technique, (iii) the PP technique yields consistent results with flat saturation profiles in both the sub and the macro-pores.

Despite the initial non-water wettability distribution within rock A, primary drainage tends to allocate water in small pores and oil in large pores, resembling a water-wet configuration. The pore-network configuration coupled with the differences in wettability between the sub-pores and the macro-pores lead to an acceptable configuration of S_{wi} during primary drainage.

3.2 Results on rock B

For rock B, we used the same 4mm plug for both the OF and the PP techniques. The main reason is because the OF results were very different from rock A with a lot of brine trapping in macropores. Thus, it was very important to observe the effect of the porous plate technique on the same pore-network at the same voxel size resolution.
At 2 µm voxel size, the total porosity of the sample is 11.6% with 38% of it in sub-resolved pores (depicted in figure 7.).
For this sample, the OF protocols remained the same as indicated in section **2.5**. After primary drainage, we directly performed a waterflooding till ROS. After that, we performed a very fast cleaning of the sample and saturated the plug with isopropyl alcohol. We re-verified that it kept its initial permeability, then we dried the sample and installed a ceramic at the outlet (bottom of the sample). Following that, we performed a PP primary drainage with capillary pressure values equal to the equilibrium DPs measured during the OF experiments (see table 3.). The goal here is to compare on the same sample, at the same inlet pressure, the trapping between the OF and the PP techniques.
Many important observations are drawn from these experiments.

Table 3. Flow parameters for OF and PP techniques applied on rock B

OF Capillary numbers **B-OF**	OF DPs equilibrium (bars) **B-OF**	PP Capillary pressure steps (bars) **B-PP**
$Ca_1 = 1.7x10^{-6}$	2.5	2.1
$Ca_2 = 3.4x10^{-6}$	4.3	4.4
$Ca_3 = 1.0x10^{-5}$	9.5	9.2
$Ca_4 = 1.7x10^{-5}$	12.8	12.6

B-OF images clearly show brine blobs trapped in macropores as illustrated in figure 12.

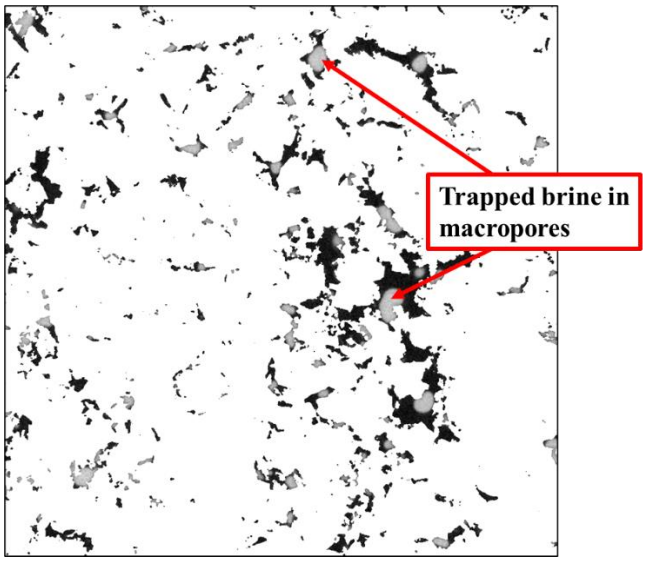

Fig. 12. Macropores of B-OF after primary drainage. Grains and sub-resolved porosity are masked (white). Oil in macropores is black and brine is the intermediate greyscale value.

We observed a lot of trapping of brine in macropores during OF compared to rock A where there was very limited trapping for high S_{wi}. Visual contact angles are also providing a very clear information: the macropores are not water wet. Surprisingly, we have very limited amount of trapped brine in macropores for sample B-PP despite the same inlet pressures used (see table 2 and figure 13). The global saturation of B-PP is almost 10 units lower than B-OF with the main decrease observed in the macropores.

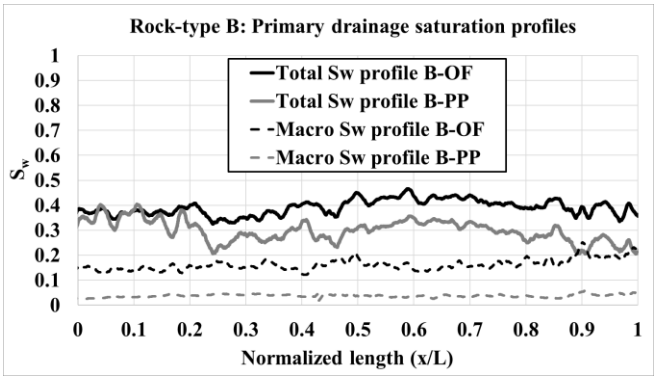

Fig. 13. Macropores of B-OF after primary drainage. Grains and sub-resolved porosity are masked (white). Oil in macropores is black and brine is the intermediate greyscale value.

We do not see any noticeable capillary end effect either in the OF or the PP experiments (macropores and sub-pores). The larger part of S_{wi} is held in the sub-pores for both experiments (88% for PP, and 59% for OF) with almost the same absolute

average saturation value in the sub-pores (see Table 2). The main difference comes from the macropores trapping.
We investigated the pore occupancy comparison of macropores after primary drainage for both OF and PP primary drainage (figure 14.). Statistically, brine is trapped in a wide range of pore sizes till very big pores during OF primary drainage, while for PP, brine is only trapped in the small pores similar to a water-wet case. This observation confirms the results that were obtained by [**1**] on the oil-wet Bentheimer samples. The PP technique avoids the trapping of brine and the pore occupancy obtained is in line with that expected for a water wet sample: brine in small pores and oil in big pores.

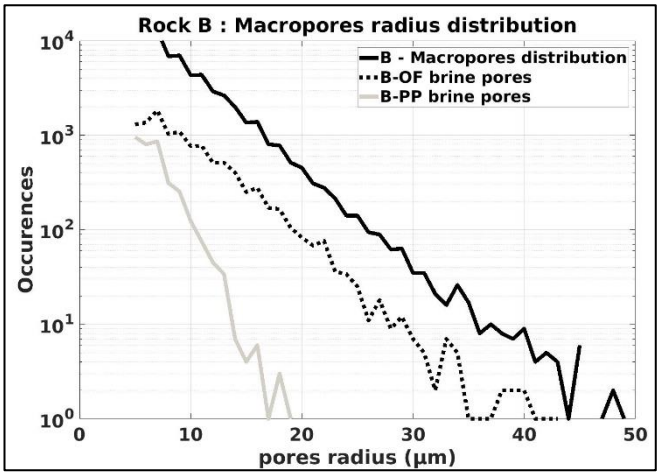

Fig. 14. Pore occupancies during primary drainage (OF & PP) of rock B

Differently from bentheimer sandstone experiments, this time we imposed for PP primary drainage, capillary pressure steps equal to the equilibrium DP values obtained during the OF primary drainage on the same plug, to be consistent with the applied pressures on the sample, mainly at the inlet. At this stage, the differences observed in trapping between OF and PP on the same sample could arise from 2 different aspects:

(i) Pressure build-up behind and at the saturation front: When performing OF primary drainage at constant rates, the pressure gradient increases gradually till breakthrough then converge to an equilibrium. There is a gradual increase of viscous forces near the inlet face and through the oil cluster invading the plug. If we consider that the macropores are well connected and oil-wet, oil invades the small pores first and bypasses some blobs of brine in big pores generating brine trapping. There will be a need of high viscous forces to be able to displace the trapped brine. Later when oil rate is increased, we can imagine that large blobs of brine will be mobilized but trapped into smaller blobs such as oil trapping during imbibition of a water-wet porous media. This implies that the important part of trapping occurs at the early stages of the oil flooding. Unfortunately, we did not perform 3D images acquisitions for each OF primary drainage capillary number. But clues could be found on the B-OF primary drainage DP curves (see figure 15). We focus on the first hour where we have in sight the starting of every flowrate we used (the experiment lasted 3 hours, thus 2.5 hours for the last stage). For the 2 first and low capillary numbers, DP reached equilibrium very quick, without any noticeable peak to locate the breakthrough. We can also see that from Ca_1 to Ca_2, DP is almost multiplied by 2, following the exact multiplier between Ca_1 and Ca_2. These observations are good indications that the trapping may occur at the earlier stage of the OF primary drainage in Ca_1 and it does not change that much with Ca_2. When increasing more the capillary number, we can see that this trend is not anymore respected thus part of the trapped brine may be produced or the new trapping distribution generated could make the DP to vary.

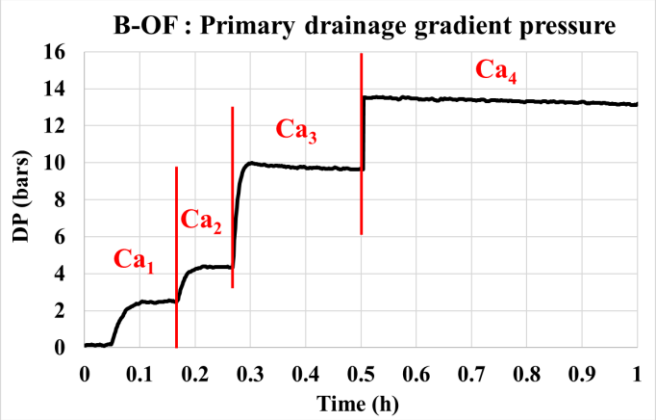

Fig. 15. Gradient pressure curve during primary drainage of B-OF. $Ca_{1\to4}$ are the different capillary numbers used on B-OF. They are reported in table 3.

(ii) Saturation of the diffusers VS rock wettability: Nono *et al.*[2] have showed that the efficiency of saturating the diffuser with the displacing fluid was also function of the rock's wettability. If the wettability of the plug is to the displacing fluid, then spontaneous displacement is prone to happen more than the low rate forced displacement near the rock-diffuser contact. This effect will generate counter-current flow of the displaced phase towards the inlet diffuser and trap a volume of this displaced phase in the diffusers' dead volumes. When reversing the flow at higher rates, this trapped non-wetting phase could be re-injected and trapped in the rock's pore network. Depending on the diffuser's geometry and dead volume, this trapped volume could be more or less important. This behavior is emphasized when dealing with mini plugs. To quantify this uncertainty, we measured effective oil permeability before and after flow reversal. We went from 10.1+/-0.3 mD to 9.2+/-0.3 mD after reversal which makes a loss of about 9%+/-6% which may be low at 3% but not negligible at 15%. We must also keep in mind that in this case, there can also be the impact of large clusters that are dislocated and redistributed in many pores.

As we did not observe a capillary end-effect in the saturation profile of the sub-pores, rock B may have a sub-porosity which is less water-wet than rock A.

4 Conclusions

In this study, we investigated at the pore scale, comparisons between two initialization techniques: the porous plate and

the oil flooding techniques, applied on reservoir rocks which are not water-wet before primary drainage.

The reservoir rocks used in this study presented a non-negligible amount of sub-resolved porosity at our voxel size images resolution. Many important observations are drawn from these experiments:

- Despite a non-water-wet behaviour, fluids distribution during primary drainage could follow a water-wet pore occupancy. This is counter-intuitive, but it depends on: (i) how wettability is distributed in the pore network. In this study, the sub-resolved pores seemed to be water-wet or at least less oil wet than the macropores, (ii) the level of wettability alteration for each network: rock B had more trapping with possibly a sub-resolved wettability which is more altered than that of rock A, (iii) How the different pore networks connect to each other. In this study, the macropores were similarly connected at almost 70% for both samples
- The porous plate technique applied first, leads to smaller values of S_{wi} than the oil flooding technique. This may be due to two different aspects: (i) the differences of pressure build-up during the invasion of the displacing phase, (ii) re-injection of the non-wetting phase which is trapped in the diffuser's dead volumes when performing flow reversal during OF technique.
- The DRP tool can be used very easily to give quick insights about these possible artifacts and provide good idea to tackle these issues for each reservoir rock case that may exhibit complex structures and deposits.

We thank TotalEnergies for their financial support and the permission to publish this paper. We also acknowledge Ms Isabelle Jolivet for providing the SEM analysis used in this paper.

References

1. F. Nono, C. Caubit, and R. Rivenq, 'Initial states of core flooding techniques evaluation: a global pore-scale investigation', International Symposium of Core Analysts, Austin, Texas, [2022] (SCA2022-16).
2. F. Nono, P. Moonen, H. Berthet and R. Rivenq, 'Multiphase flow imaging through X-ray microtomography: Reconsideration of capillary end effects and boundary conditions', International Symposium of Core Analysts, Pau, France [2019] (SCA2019-019).
3. D.B. Bennion, F.B. Thomas, and T. Ma, 'Determination of Initial Fluid Saturations Using Traced Drilling Media', Journal of Canadian Petroleum Technology, 40, [2001].
4. J. Reed, S. Pruno, I. Zubizarreta and R. Johansen, 'Causal protocols to assess the viability of native state or restored state preparation', International Symposium of Core Analysts, Austin, Texas, [2022] (SCA2022-28).
5. R. Farokhpoor, L. Sundal, A. Skjaerstein, A. Hebing, X. Zhang and L. Pirlea, 'Core cleaning and wettability restoration – selecting appropriate method', International Symposium of Core Analysts, [2021] (SCA2021-016).
6. O. Vizika, J.P. Duquerroix, 'Gas injection and Heterogeneous Wettability: what is the relevant information that petrophysics can provide', International Symposium of Core Analysts, Calgary, Canada, [1997] (SCA-9708).
7. G. Garfi, C.M. John, M. Ruecker, Q. Lin, C. Spurin, S. Berg and S. Krevor, 'Determination of the spatial distribution of wetting in the pore networks of rocks', Journal of Colloid and Interface Science 613, 786-795, [2022].
8. S. Foroughi, B. Bijeljic, Q. Lin, A. Raeini, M. Blunt, pore-by-pore modeling, analysis, and prediction of two-phase flow in mixed-wet rocks, Physical Review E. 102.10.1103/PhysRevE.102.023302, [2020].
9. C.A. McPhee, and K.G. Arthur, 'Relative Permeability Measurements: An Inter-Laboratory Comparison', Paper presented at the European Petroleum Conference, London, United Kingdom, October 1994. doi: https://doi.org/10.2118/28826-MSC.A.McPhee & K.G. SPE 28826.
10. V. Fernandes, C. Caubit, B. Nicot, F. Pairoys, H. Bertin, J. Lachaud, 'Hybrid technique for setting initial water saturation on core samples', International Symposium of Core Analysts, Austin, Texas, [2022] (SCA2022-23).
11. Wilson O.B., Tjetland B.G. and Skauge A., "Porous plates influence on effective drainage rates in capillary pressure experiments", International Symposium of Core Analysts, Edinburg, Scotland [2001] (SCA2001-30).
12. Z. Zubo, L. Manli and C. Weifeng, "An Experimental Study of Irreducible Water Saturation Establishment", International Symposium of Core Analysts, Avignon, France, [2014] (SCA2014-070).
13. M. Fleury, "The spinning porous plate (SPP) method: a new technique for setting irreducible water saturation on core samples", International Symposium of Core Analysts, Noordwijk, Netherlands, [2009] (SCA2009-08).
14. Q. Lin, Y. Al-khulaifi, B. Bijeljic and M.J. Blunt, [2016]. 'Quantification of sub-resolution porosity in carbonate rocks by applying high-salinity contrast brine using X-ray microtomography differential imaging', Advances in Water Resources. 96. 10.1016/j.advwatres.2016.08.002.
15. Q. Lin, B. Bijeljic, H. Rieke and M.J. Blunt, [2017]. 'Visualization and quantification of capillary drainage in the pore space of laminated sandstone by a porous plate method using differential imaging x-ray microtomography'. Water Resources Research 53, 7457–7468.
16. A.Q. Raeini, B. Bijeljic, M.J. Blunt, 'Generalized network modelling: capillary-dominated two-phase flow – model description'. Physical review E. 97 10.1103/PhysRevE.97.023308, [2017].